Microchimica Acta (2019) 186: 4
https://doi.org/10.1007/s00604-018-3060-7

ORIGINAL PAPER

A triazine based organic framework with micropores and mesopores for use in headspace solid phase microextraction of phthalate esters

Huihua Guo [1] · Gang Chen [1] · Jiutong Ma [1] · Qiong Jia [1]

Received: 13 June 2018 / Accepted: 18 October 2018 / Published online: 7 December 2018

Abstract

A dual-pore covalent organic framework (COF) that contains micropores and mesopores was prepared from 2,4,6-triphenoxy-1,3,5-triazine (TPT). A building block is used in which double linking sites were introduced at each branch of a C_3-symmetric skeleton. The COF is shown to be a viable coating for fibers for solid-phase microextraction of phthalic acid esters (PAEs). Its high specific surface, high hydrophobicity, and wide pore size distribution of a TPT-COF coated fiber result in extraordinarily powerful extraction of PAEs. The enrichment factor is up to 7790 under optimum conditions. The method has detection limits that range between 5 and 95 ng L^{-1}. The inter-batch relative standard deviations are between 3.1 and 10.9%, and those for intra-batch assays are from 0.8 to 4.7%. The TPT-COF coated fibers were applied to the extraction of PAEs from (spiked) juice samples, and satisfactory recoveries were achieved.

Keywords Covalent organic framework · Multiple-linking-site · SPME · Gas chromatography

Introduction

Phthalate esters (PAEs) are widely used as plasticizers in plastics products to improve their flexibility [1, 2]. PAEs and their metabolites are carcinogenic and endocrine-disrupting chemicals, which have adverse health effects on mammals. Therefore, developing effective and fast methods is important for measuring PAEs in food and environment samples. However, the concentrations of PAEs in complex matrices are unusual low. Sample pretreatment and enrichment processes are crucial steps to obtain accurate results before instrumental analysis.

Several pretreatment methods have been developed for PAEs such as liquid-liquid microextraction (LLME) [3, 4], magnetic solid phase extraction (MSPE) [5] and solid-phase microextraction (SPME) [6, 7]. Among them, SPME integrates sampling, isolation, and enrichment into a single step [8]. SPME is based on the extraction equilibrium of the analytes between fiber and sample matrix. The property of the fiber is critical to improve the extraction efficiency of SPME. Some commercial fibers have been available including polyacrylate (PA), polydimethylsiloxane (PDMS), and divinylbenzene/carboxen/polydimethylsiloxane (DVB/CAR/PDMS). However, commercial fibers suffer from the drawbacks of high cost, low thermal and chemical stability. Therefore, self-made fibers have been investigated such as graphene/poly(vinyl chloride) nanocomposite (G/PVC) [9], oxidized multi-walled carbon nanotubes-polypyrrole composite (MWCNTs-PPy) [10], carbopack Z/PDMS [2], polymeric ionic liquid (PIL) [11, 12], metal–organic frameworks (MOF) [13], metal-organic nanotubes [14], polyaniline-polypyrrole (PANI-PPY) [15] and polyethylene glycol/graphene oxide (PEG/GO) [16].

Microporous organic polymers (MOPs) are constructed by organic building blocks through strong carbon-carbon, carbon-nitrogen, and/or carbon-oxygen covalent bonds [17]. MOPs exhibit large specific surface area, low skeleton density, high water, moisture, and chemical stability. Among the various MOPs, conjugated microporous polymer (CMPs) [18], porous aromatic frameworks (PAFs) [19], hypercrosslinked-polymers (HCPs) [20], and covalent organic frameworks (COFs) [21–23] have been reported as SPME

Electronic supplementary material The online version of this article (https://doi.org/10.1007/s00604-018-3060-7) contains supplementary material, which is available to authorized users.

✉ Jiutong Ma
majt@jlu.edu.cn

[1] College of Chemistry, Jilin University, Changchun 130012, China

fiber materials. COFs-based SPME coatings are mainly focused on conventional COFs with single pores. They are usually synthesized from building blocks with C_3/D_{3h} or C_4/D_{4h} symmetry and ditopic linear linkers, which have uniform pore structures (e.g., hexagonal or tetragonal) [21].

Recently, hierarchical porous materials with highly ordered internal structures and hierarchical porosities [24, 25] were proved to be capable of greatly facilitating the extraction of the target analytes [26]. These COFs opened a gallery for the application of hierarchical COFs in the field of separation and enrichment. Generally speaking, there are three synthetic units for constructing hierarchical COFs [27], i.e., synthesized by cyclic building blocks with intrinsic pores or by noncyclic building blocks, and constructed by a multiple-linking-site building block including two linking sites at each branch of the original skeleton. The former two methods suffer from the disadvantages that only one pore can be detectable. This is because small pores in the cyclic monomers or the structures of the COFs cannot be predicted raised by the two types of topological structures products. When a multiple-linking-site building block is used, heteroporous COFs can be produced without formation of any COF isomers.

In this work, a multiple-linking-site building block was used for constructing dual-pore COFs. 2,4,6-triphenoxy-1,3,5-triazine (TPT) based multiple-linking-site building block was prepared with cyanuric chloride and dimethyl 5-hydroxyisophthalate. The dual-pore COF material was employed as a SPME fiber for the enrichment of PAEs in juice samples combing with GC-FID. The TPT-COF material include abundant C=N and C=C groups, which may facilitate the extraction of PAEs relying on π stacking interactions. Furthermore, the dual structure is expected to be beneficial to adsorb the targets according to Yin et al.'s work [26].

Experimental section

Materials and apparatus are supplied in Electronic Supporting Material. The TPT-COOEt was synthesized according to a previous literature [28]. 4.5 mmol of dimethyl 5-hydroxyisophthalate was dissolved in 15 mL of DMF, to which 9 mmol of potassium carbonate and 1 mmol of cyanuric chloride were added. Then the reaction mixture was refluxed for 48 h. After completion of the reaction, the mixture was cooled to room temperature and then filtered. The solid residue was washed with acetone and then the yellow filtrate was evaporated to dryness. The obtained residue was washed with 10% $NaCO_3$ to obtain the yellow solid building block, TPT-COOEt.

TPT-CON_2H_4 was synthesized according to a previous literature [29] with a modified procedure. 0.73 mmol of TPT-COOEt was added into a 100 mL round bottom flask containing 45 mL of ethanol and 6 mL of hydrazine hydrate. The mixture was stirred and heated to reflux for 12 h. After cooled, the white crystals precipitate was isolated by filtration, and then washed thoroughly with water and ethanol. Finally, the white solid was dried to obtain the desired product.

TPT-COF was synthesized under solvothermal conditions according to previous reports [30]. Firstly, 15 mmol of TPT-CON_2H_4 in 3 mL of mesitylene/dioxane (1:1), 0.45 mmol of *p*-phthalaldehyde in 3 mL of mesitylene/dioxane (1:1) and 0.5 mL of 9 mol L^{-1} aqueous acetic acid was mixed. The mixture was sonicated for 3 min, then transferred into a Teflon-lined stainless-steel autoclave and heated at 120 °C for 72 h. The precipitate was collected by filtration and washed with anhydrous dioxane, THF, and acetone successively. Finally, the collected powder was dried in vacuum overnight to yield the yellow product, TPT-COF.

Preparation of the SPME fiber

A 5 μL GC micro-syringe was used to make the self-made SPME device, which was shown in Fig. 1. Firstly, one side of the stainless-steel wire (1.0 cm long) of the micro-syringe was corroded with aqua regia about 30 min. The wire was polished, washed in an ultrasonic bath with acetone, ethanol, distilled water, and dried at room temperature. Secondly, the polished stainless steel was inserted into epoxy resin glue, pulled out quickly. The excessive epoxy resin glue was wiped by a thin layer of glass sheet. Finally, the stainless-steel wire was vertically inserted into a centrifuge tube with the TPT-COF powder and then rotated several cycles. After solidification at room temperature for 24 h, the coated fiber was placed in an oven at 120 °C for 30 min. This process was carried out three times and the redundant TPT-COF powder was removed by pushing and pulling the SPME holder for several times.

Analysis of PAEs coupled with SPME procedure

Juice samples provided were bought from local markets. The samples were filtered through a 0.45 μm membrane filter and stored at 4 °C in a refrigerator until analysis.

Prior to the SPME procedure, the TPT-COF fiber was aged in the GC injection at 250 °C for 30 min to avoid any contamination. All experiments were performed in headspace solid phase microextraction (HP-SPME). PAEs were extracted in a 20-mL amber vial enclosed by a PTFE-coated septum including 1 mL of working solutions. Then, the prepared vial with a 1-cm long Teflon-coated stirring bar was placed in the magnetic stirrer. The stirrer was used to control the extraction temperature and agitation speed. Next, extractions were carried out by exposing the fiber into the vial and fixed the fiber

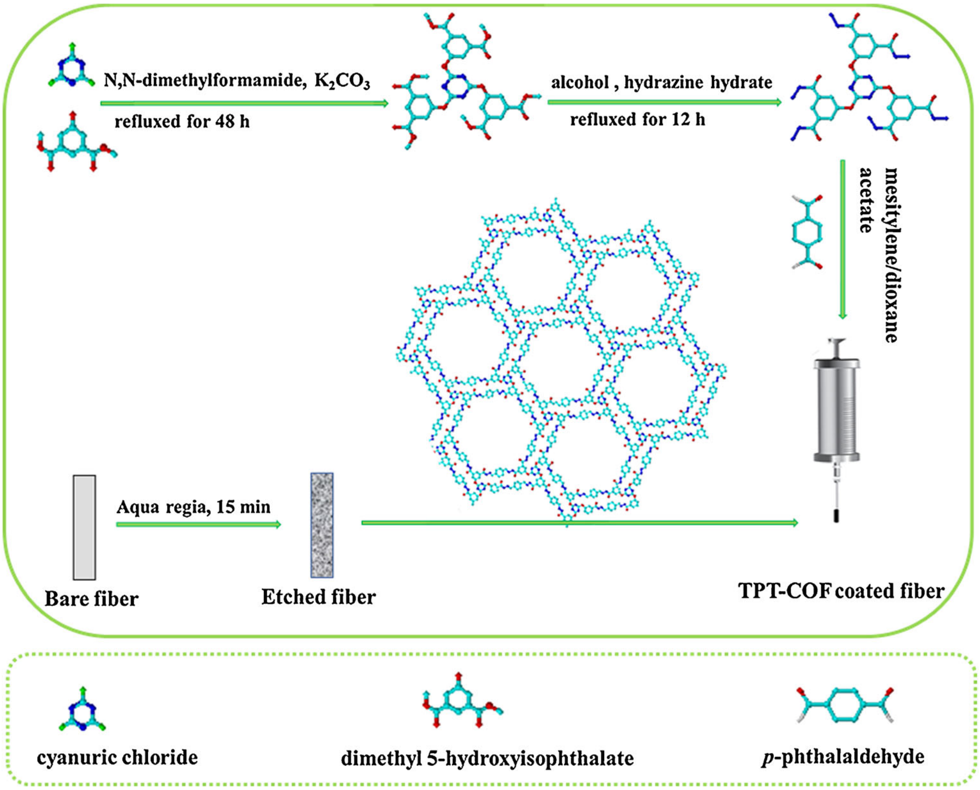

Fig. 1 Schematic fabrication process of SPME fiber coated with the 2,4,6-triphenoxy-1,3,5-triazine based covalent organic framework (TPT/COF)

above the juice sample. After a certain period of time, the fiber was removed from the vial and immediately introduced into the GC inlet for thermal desorption.

Results and discussion

Choice of materials

The 2,4,6-triphenoxy-1,3,5-triazine based covalent organic framework (TPT/COF) exhibits many desirable properties, such as high surface area, good thermal stability and inherent porosity. The high surface area and porosity with hierarchical may improve the extraction efficiency of analytes. TPT-COF combines triazine ring and benzene rings, which can offer strong π-stacking interactions with the compounds containing abundant π-electrons [31, 32]. Based on these considerations, TPT-COF can be expected as an attractive and potential material for SPME.

Characterization of the TPT-COF coated fiber

FT-IR spectra analyses were performed to confirm the structure of TPT-COF. FT-IR spectra of cyanuric chloride, dimethyl 5-hydroxyisophthalate, and TPT-COOEt are shown in Fig. S1 (Electronic Supplementary Material). The adsorption band at 854 cm^{-1} in cyanuric chloride corresponded to C–Cl vibrations. The adsorption band at 3362 cm^{-1} is attributed to O–H stretching vibrations of dimethyl 5-hydroxyisophthalate. However, these bands disappeared in the spectrum of TPT-COOEt, suggesting that 5-hydroxyisophthalate was converted. In Fig. 2a, an adsorption band at 3323 cm^{-1} existed in the spectrum of TPT-CON_2H_4, which corresponded to N–H stretching vibrations of amide linkage in TPT-CON_2H_4. The band vanished in the spectrum of TPT-COF while a new band at 1563 cm^{-1} appeared owing to C=N stretching vibrations, demonstrating the successful synthesis of TPT-COF. In addition, the peak at 1654 cm^{-1} is attributed to the stretching vibrations of the C=O band. The peak was a result of the blue shift from the bands of TPT-CON_2H_4 (1635 cm^{-1}). This blue shift can be attributed to the attenuation of the stretching vibrations of C=O band from the adjacent imine bonds [29].

TGA analysis under nitrogen atmosphere at the heating rate of 10 °C min^{-1} over the temperature range of 20–900 °C (Fig. 2b) was carried out to evaluate the thermal stability of the prepared TPT-COF. Results show that there was a little mass loss before 100 °C due to the loss of adsorbed water. Further heating show no obvious weight loss until the material decomposed at 340 °C approximately. These results indicate that TPT-COF can resist the high temperature of GC injector when the TPT-COF coated fiber was introduced for desorption.

A key evidence for the formation of dual-pore COF was provided by N_2 extraction-desorption experiments (Fig. 2c). The whole curve exhibit type I and IV shapes at low and high relative pressure, respectively, indicating that this material possessed both microporous and mesoporous characteristics.

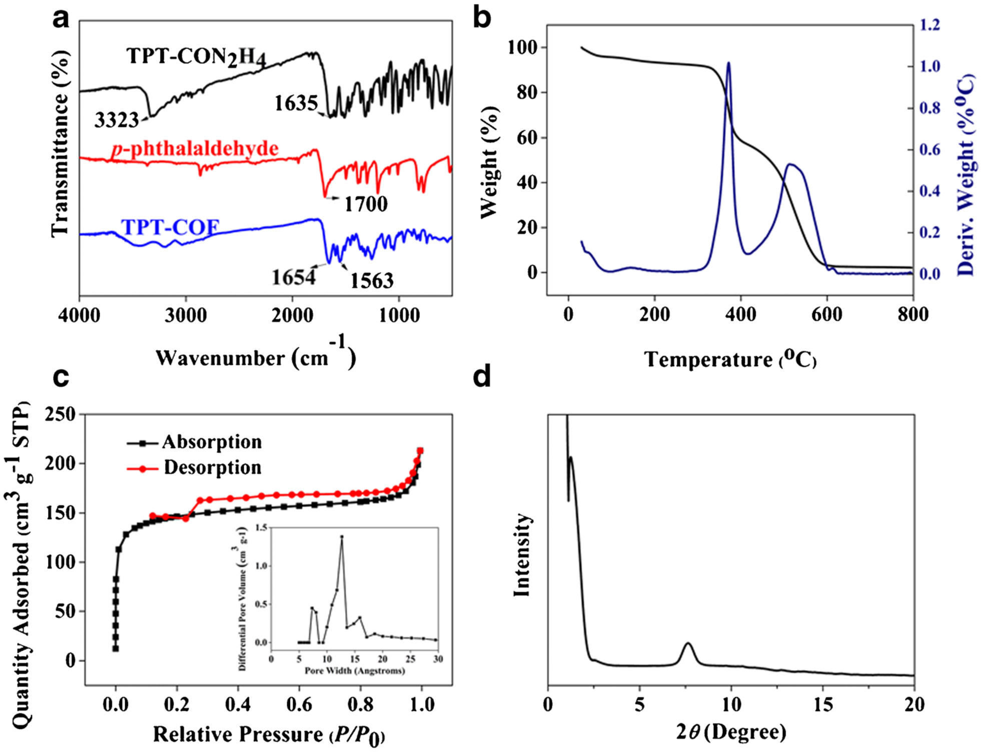

Fig. 2 **a** FT-IR spectra of TPT-CON$_2$H$_4$, *p*-phthalaldehyde, and TPT-COF; **b** TG-DTG curves of TPT-COF; **c** N$_2$ adsorption-desorption isotherm curves of TPT-COF. Inset: pore size distribution profile; and **d** PXRD pattern of TPT-COF

The Brunauer-Emmett-Teller (BET) surface area was calculated to be about 485 cm^2 g^{-1}. The pore size distribution profiles reveal that the material exhibited two main pore sizes at 7.5 Å and 12.6 Å, respectively. Moreover, the experimental PXRD pattern display a strong peak at 1.25°nd a weak signal at 7.66° (Fig.2d). The results represent that the prepared material was a dual-pore crystal material. In addition, the morphology (Fig. S2, Electronic Supporting Material) indicates that the crystal TPT-COF with a layer-by-layer structure was fixed on SSF successfully. The coating possesses a homogeneous surface and the thickness of is about 10 μm.

Optimization of HS-SPME conditions

Several experimental parameters affecting the extraction efficiency of the self-made TPT-COF coating were studied. Experimental parameters include extraction time, extraction temperature, salt concentration, and desorption time. These parameters were investigated and optimized to achieve the best enrichment. The following experimental conditions were determined to be optimum: extraction time of 40 min, extraction temperature of 85 °C, ionic strength of 20% (*w*/*v*), and desorption time of 6 min. Relevant experimental data are given in Fig. S3 (Electronic Supporting Material).

Under the optimized extraction conditions, the extraction capacity of the TPT-COF coated fiber toward the target PAEs was investigated. As shown in Fig. S2, the extraction capacities of DMP, DEP, DPRP, DAP, DBP, DIOP, DCHP, DnDP, and DPhP were found to be 533, 2215, 25,012, 10,720, 12,580, 841, 625, 847, and 683 ng, respectively. Relevant experimental data are given in Fig. S4 (Electronic Supplementary Material).

Method validation

The analytical features of PAEs with the HS-SPME-GC-FID method were studied under the optimized conditions. As shown in Table 1, the linear ranges are 0.1–100 μg L^{-1} for DMP, DEP, DNDP, DPHP, 0.05–50 μg L^{-1} for DCHP, and 0.01–50 μg L^{-1} for DPP, DAP, DBP, and DEHP. All of the target compounds show good linearity with the relation coefficients (*r*) ranged from 0.9906 to 0.9988. The limits of detection (LODs) and limits of quantification (LOQ), determined based on a signal-to-noise ratio (*S*/*N*) of 3:1 and 10:1, were in the range of 0.01–0.10 μg L^{-1} and 0.02–0.31 μg L^{-1}, respectively. The relative standard deviations (RSDs) for nine replicates of extraction of PAEs using one fiber were lower than 4.72%. The fiber-to-fiber reproducibility evaluated using three fibers were from 3.08% to 10.90%. Moreover, the enrichment factors (EFs) ranged from 10 to 7790, which were defined as the ratio of sensitivity of the target compounds after extraction to that before extraction.

The lifetime of a fiber is very important for practical application and was investigated by extracting PAEs. As shown in Fig. S5 (Electronic Supplementary Material), the self-made fiber was used more than 55 cycles for the extraction/desorption of the target compounds without significant

Table 1 Analytical performance for GC-FID determination of PAEs using TPT-COF coated fiber

Analyte	LR (μg L^{-1})	LOD (μg L^{-1})	RSD		EF
			Intra-batch (%, $n = 3$)	Inter-batch (%, $n = 5$)	
DMP	0.1–100	0.10	4.72	7.96	10
DEP	0.1–100	0.10	3.20	9.73	221
DPP	0.01–50	0.07	4.67	6.48	3098
DAP	0.01–50	0.01	1.25	3.28	5557
DBP	0.01–50	0.01	0.83	4.39	7790
DEHP	0.01–50	0.01	1.23	3.08	1768
DCHP	0.05–50	0.06	4.31	7.63	395
DNDP	0.1–100	0.07	2.65	8.94	132
DPHP	0.1–100	0.07	3.23	10.90	113

decrease in the extraction ability, indicating the high durability of the fiber.

Extraction mechanism

TPT-COF had different capacities for the target PAEs, which probably originated from dissimilar extraction mechanisms. As shown in Table 1 and Table S1, the logK_{ow} values of DMP, DEP, DPP, DBP, DEHP, and DNDP increased gradually. Under this condition, the extraction affinities of them with the TPT-COF coated fiber were mostly proportional to the hydrophobicity of the targets. Therefore, the extraction impetus is the "hydrophobic-hydrophobic" interaction between TPT-COF and the hydrophobic PAEs [19]. It should be noted that although DEHP and DNDP exhibited higher logK_{ow} values, EFs of them became lower, which might be because small molecules were more apt to enter into the pores of the TPT-COF fiber [33]. Similarly, the EFs of DCHP and DPHP were low, which was also due to the size effect [34]. In addition, DAP has slightly smaller logK_{ow} value than DPP but its EF is higher, indicating that π stacking effect also made contribution to the extraction of DAP by the TPT-COF coated fiber [35].

Comparative study

To evaluate the extraction ability of TPT-COF toward the target compounds, a commercial polydimethylsiloxane (PDMS) fiber was selected for comparison. As shown in Fig. 3, the self-made fiber possessed extraction efficiencies that are better by factors between 1.08 and 40.7 than those obtained by PDMS fiber. The high extraction capacity of the TPT-COF coated fiber for PAEs was presumably attributed to the strong interactions as mentioned above.

A comparison of the present strategy with some reported methods which have been applied to the analysis of the target

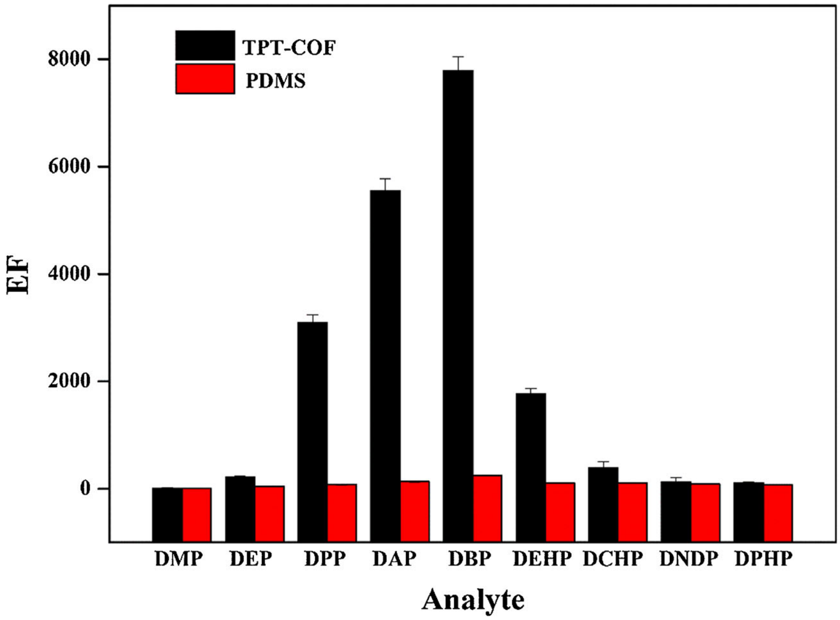

Fig. 3 Comparison of enhancement factors of PAEs with TPT-COF and PDMS fibers

PAEs was summarized in Table S2 (Electronic Supplementary Material). Although the LOD values of the present method were not lowest, the TPT-COF coated SPME fiber showed high enrichment efficiency for PAEs, implying its great potential for application in the area of sample pretreatment.

Application to real samples

To evaluate the practicality of the developed method, three juice samples bought from local market were analyzed under the optimized experimental conditions. 1 mL juice samples were spiked with two concentrations, 0.5 μg L^{-1} (Level 1) and 1 μg L^{-1} (Level 2). Typical chromatograms were displayed in Fig. S6 (Electronic Supplementary Material). As shown in Table S3 (Electronic Supplementary Material), the recoveries located in the ranges of 80.6%–108.9% (0.5 μg L^{-1}) and 79.4%–110.3% (1 μg L^{-1}) for the studied analytes. The satisfactory results of recovery measurements confirmed that the established method was reliable.

Conclusions

In this work, a novel dual-pore TPT-COF-based SPME fiber was successfully prepared and characterized by FT-IR, TGA, BET, XRD, SEM, and TEM determinations. These results indicate that the TPT-COF coating is a crystal material including micropores and mesopores. The developed HS-SPME-GC-FID method exhibits low LOD values and wide linear ranges when used for the determination of PAEs. Based on results of EFs by two fibers (TPT-COF coated fiber and commercial PDMS fiber) toward PAEs, the self-made TPT-COF exhibited high extraction ability because of high surface area, π- interaction, and hydrophobic interactions. It can be expected that the coating exhibits extraction selectivity for the analytes containing C=C and C=N groups including some drugs, herbicides, and pesticides. Although the present dual-pore COF material cannot selectively enrich PAEs in the presence of such analytes, it opens a gallery for the wider applications of COFs to the area of SPME.

Acknowledgements The project was supported by Open Project of State Key Laboratory of Supramolecular Structure and Materials, Jilin University, China (sklssm201815).

Compliance with ethical standards The author(s) declare that they have no competing interests.

References

1. Al-Saleh I, Elkhatib R (2016) Screening of phthalate esters in 47 branded perfumes. Environ Sci Pollut Res Int 23:455–468
2. Barp L, Purcaro G, Franchina F, Zoccali M, Sciarrone D, Tranchida P, Mondello L (2015) Determination of phthalate esters in vegetable oils using direct immersion solid-phase microextraction and fast gas chromatography coupled with triple quadrupole mass spectrometry. Anal Chim Acta 887:237–244
3. Amiri A, Ghaemi F (2017) Microextraction in packed syringe by using a three-dimensional carbon nanotube/carbon nanofiber–graphene nanostructure coupled to dispersive liquid-liquid microextraction for the determination of phthalate esters in water samples. Microchim Acta 184:3851–3858
4. Jiao C, Ma R, Li M, Hao L, Wang C, Wu Q, Wang Z (2017) Magnetic cobalt-nitrogen-doped carbon microspheres for the preconcentration of phthalate esters from beverage and milk samples. Microchim Acta 184:2551–2559
5. Yamini Y, Faraji M, Adeli M (2015) Magnetic silica nanomaterials for solid-phase extraction combined with dispersive liquid-liquid microextraction of ultra-trace quantities of plasticizers. Microchim Acta 182:1491–1499
6. Hou X, Guo Y, Liang X, Wang X, Wang L, Wang L, Liu X (2016) Bis(trifluoromethanesulfonyl)imide-based ionic liquids grafted on graphene oxide-coated solid-phase microextraction fiber for extraction and enrichment of polycyclic aromatic hydrocarbons in potatoes and phthalate esters in food-wrap. Talanta 153:392–400
7. Xia S, Dong J, Chen Y, Wang Y, Chen X (2013) Three dimensional phytic acid-induced graphene as a solid-phase microextraction fiber coating and its analytical applications for nerolidol in tea. Chin Chem Lett 29:107–110
8. Wang X, Sheng WR, Jiao XY, Zhao RS, Wang ML, Lin JM (2018) Zinc(II)-based metal-organic nanotubes coating for high sensitive solid phase microextraction of nitro-polycyclic aromatic hydrocarbons. Talanta 186:561–567
9. Amanzadeh H, Yamini Y, Moradi M, Asl YA (2016) Determination of phthalate esters in drinking water and edible vegetable oil samples by headspace solid phase microextraction using graphene/polyvinylchloride nanocomposite coated fiber coupled to gas chromatography-flame ionization detector. J Chromatogr A 1465:38–46
10. Asadollahzadeh H, Noroozian E, Maghsoudi S (2010) Solid-phase microextraction of phthalate esters from aqueous media by electrochemically deposited carbon nanotube/polypyrrole composite on a stainless steel fiber. Anal Chim Acta 669:32–38
11. Ho TD, Toledo BR, Hantao LW, Anderson JL (2014) Chemical immobilization of crosslinked polymeric ionic liquids on nitinol wires produces highly robust sorbent coatings for solid-phase microextraction. Anal Chim Acta 843:18–26
12. Feng J, Sun M, Bu Y, Luo C (2015) Facile modification of multi-walled carbon nanotubes-polymeric ionic liquids-coated solid-phase microextraction fibers by on-fiber anion exchange. J Chromatogr A 1393:8–17
13. Zhang B, Xu G, Li L, Wang X, Li N, Zhao RS, Lin J (2018) Facile fabrication of MIL-96 as coating fiber for solid-phase microextraction of trihalomethanes and halonitromethanes in water samples. Chem Eng J 350:240–247
14. Li QL, Huang F, Wang XL, Wang X, Zhao RS (2017) Multiple-helix cobalt(II)-based metal-organic nanotubes on stainless steel fibers for solid-phase microextraction of chlorophenol and nitrophenols from water samples. Microchim Acta 184:1817–1825
15. Zhao S, Wu M, Zhao F, Zeng B (2013) Electrochemical preparation of polyaniline-polypyrrole solid-phase microextraction coating and its application in the GC determination of several esters. Talanta 117:146–151

16. Hou X, Yu H, Guo Y, Liang X, Wang S, Wang L, Liu X (2015) Polyethylene glycol/graphene oxide coated solid-phase microextraction fiber for analysis of phenols and phthalate esters coupled with gas chromatography. J Sep Sci 38:2700–2707
17. Zhang Y, A S ZY, Luo X, Li Z, Xia H, Liu X, Mu Y (2014) Gas uptake, molecular sensing and organocatalytic performances of a multifunctional carbazole-based conjugated microporous polymer. J Mater Chem A 2:13422–13430
18. Meng WK, Liu L, Wang X, Zhao RS, Wang ML, Lin JM (2018) Polyphenylene core-conjugated microporous polymer coating for highly sensitive solid-phase microextraction of polar phenol compounds in water samples. Anal Chim Acta 1015:27–34
19. Jin Y, Li Z, Yang L, Xu J, Zhao L, Li Z, Niu J (2017) Porous aromatic framework 48/gel hybrid material coated solid-phase microextraction fiber for the determination of the migration of styrene from polystyrene food contact materials. Anal Chem 89:1290–1298
20. Liu S, Chen D, Zheng J, Zeng L, Jiang J, Jiang R, Zhu F, Shen Y, Wu D, Ouyang G (2015) The sensitive and selective adsorption of aromatic compounds with highly crosslinked polymer nanoparticles. Nanoscale 7:16943–16951
21. Wu M, Chen G, Liu P, Zhou W, Jia Q (2016) Polydopamine-based immobilization of a hydrazone covalent organic framework for headspace solid-phase microextraction of pyrethroids in vegetables and fruits. J Chromatogr A 1456:34–41
22. Zhang S, Yang Q, Li Z, Wang W, Wang C, Wang Z (2017) Covalent organic frameworks as a novel fiber coating for solid-phase microextraction of volatile benzene homologues. Anal Bioanal Chem 409:3429–3439
23. Guo H, Chen G, Wu M, Ma J, Jia Q (2017) Preparation of a porous aromatic framework via the Chan-Lam reaction: a coating for solid-phase microextraction of antioxidants and preservatives. Microchim Acta 184:4409–4416
24. Zhu Y, Wan S, Jin Y, Zhang W (2015) Desymmetrized vertex design for the synthesis of covalent organic frameworks with periodically heterogeneous pore structures. J Am Chem Soc 137:13772–13775
25. Zhou TY, Xu SQ, Wen Q, Pang ZF, Zhao X (2014) One-step construction of two different kinds of pores in a 2D covalent organic framework. J Am Chem Soc 136:15885–15888
26. Yin ZJ, Xu SQ, Zhan TG, Qi QY, Wu ZQ, Zhao X (2017) Ultrahigh volatile iodine uptake by hollow microspheres formed from a heteropore covalent organic framework. Chem Commun 53:7266–7269
27. Qian C, Xu SQ, Jiang GF, Zhan TG, Zhao X (2016) Precision construction of 2D heteropore covalent organic frameworks by a multiple-linking-site strategy. Chem Eur J 22:17784–17789
28. Xu L, Ding SY, Liu J, Sun J, Wang W, Zheng QY (2016) Highly crystalline covalent organic frameworks from flexible building blocks. Chem Commun 52:4706–4709
29. Ding SY, Dong M, Wang YW, Chen YT, Wang HZ, Su CY, Wang W (2016) Thioether-based fluorescent covalent organic framework for selective detection and facile removal of mercury(II). J Am Chem Soc 138:3031–3037
30. Li Y, Yang CX, Yan XP (2017) Controllable preparation of core-shell magnetic covalent-organic framework nanospheres for efficient adsorption and removal of bisphenols in aqueous solution. Chem Commun 53:2511–2514
31. Wang W, Li Z, Wang W, Zhang L, Zhang S, Wang C, Wang Z (2017) Microextraction of polycyclic aromatic hydrocarbons by using a stainless steel fiber coated with nanoparticles made from a porous aromatic framework. Microchim Acta 185:1–10
32. Wen CY, Chen J, Li M, Xue Y, Aslam S, Subhan F, Zhao R, Yu J, Zeng J, Chen X (2017) Gold nanoparticles deposited on mesoporous carbon as a solid-phase sorbent with enhanced extraction capacity and selectivity for anilines. Microchim Acta 184:3929–3936
33. He J, Lv R, Zhu J, Lu K (2010) Selective solid-phase extraction of dibutyl phthalate from soybean milk using molecular imprinted polymers. Anal Chim Acta 661:215–221
34. Yang J, Li Y, Wang Y, Ruan J, Zhang J, Sun C (2015) Recent advances in analysis of phthalate esters in foods. Trac-Trend Anal Chem 72:10–26
35. Ye CW, Gao J, Yang C, Liu XJ, Li XJ, Pan SY (2009) Development and application of an SPME/GC method for the determination of trace phthalates in beer using a calix[6]arene fiber. Anal Chim Acta 641:64–74